

3D Printing Natural Organic Materials by Photochemistry

Joyce Laura Da Silva Gonçalves¹, Silvano Rodrigo Valandro¹, Hsiu-Fen Wu³, Yi-Hsiung Lee³, Bastien Mettra², Cyrille Monnereau², Carla Cristina Schmitt Cavalheiro¹, Agnieszka Pawlicka¹, Monica Focsan⁴, Chih-Lang Lin³, Patrice L. Baldeck^{*1-2}

¹IQSC-USP, Av. Trabalhador São-carlense 400, 13566-590 São Carlos-SP, Brazil.

²Univ. Lyon, ENS de Lyon, CNRS, Université Lyon 1, Laboratoire de Chimie, Lyon, France.

³Inst. of Biomed. Eng. and Mater. Sci., Cent. Taiwan Univ. of Sci. and Tech., Taichung 406, Taiwan.

⁴Interdisciplinary Research Inst. on Bio-NanoSciences, Babes-Bolyai Univ., Cluj-Napoca, Romania

*E-mail: patrice.baldeck@ens-lyon.fr (permanent address)

ABSTRACT

In previous works, we have used two-photon induced photochemistry to fabricate 3D microstructures based on proteins, anti-bodies, and enzymes for different types of bio-applications. Among them, we can cite collagen lines to guide the movement of living cells, peptide modified GFP biosensing pads to detect Gram positive bacteria, anti-body pads to determine the type of red blood cells, and trypsin columns in a microfluidic channel to obtain a real time biochemical micro-reactor. In this paper, we report for the first time on two-photon 3D microfabrication of DNA material. We also present our preliminary results on using a commercial 3D printer based on a video projector to polymerize slicing layers of gelatine-objects.

Keywords: two-photon polymerization, 3D printing, DNA, BSA, gelatine

1. INTRODUCTION

1.1 3D printing natural organic materials

The 3D printing of natural, organic, and biodegradable molecules and macromolecules is important not only for biomedical applications, but also to develop green 3D water-based processes. For example, polylactic acid is a thermoplastic polyester derived from cornstarch, tapioca roots, or sugar cane, and one of the rare bioplastics that can be used in fused deposition modeling (FDM) 3D printing. On the other hand, most organic materials are sensitive to heat treatment; therefore, 3D printing processes of natural macromolecules, which uses photochemistry to crosslink their chains dispersed in water solutions is most likely appropriate. Early works on photo-crosslinking of polysaccharides (alginate, chitosan, hyaluronic acid, etc.) targeted a fabrication of drug microcapsules and biodegradable scaffolds by free radical polymerization. Recently, researches on two-photon induced photochemistry have demonstrated the fabrication of bioactive 3D microstructures with proteins. [1-2] Photo-induced cross-linking of proteins is obtained by photo-oxidation and then condensation of some of their amino acid residues. Our previous works include a microfabrication of collagen lines to guide a movement of living cells, peptide modified GFP bio-sensing pads for Gram positive bacteria detecting, anti-body pads for type of red blood cells determination, and trypsin columns in a microfluidic channel for a real time biochemical micro-reactor 3D. [3-8]

In this work, we report for the first time on 3D photo-induced cross-linking of DNA material. Some reports on thin films of DNA from salmon waste have shown that it has excellent optical and electronic properties. [9] Moreover, it has been reported that photo-crosslinking of spin-coated DNA thin films improved its opto-electronic properties. [10-11] Here, we demonstrate a possibility to fabricate 3D micro-objects for micro-optics application from DNA. In addition, we present our preliminary results on using a commercial 3D printer, based on a digital light projector, to fabricate objects with high concentrations of BSA or gelatin.

2. MATERIALS AND METHODS

2.1 Preparation of photosensitive DNA and protein solutions

- Photosensitive DNA solution:

DNA stock aqueous solution was prepared by dissolving 0.22 g of DNA ($MW=8 \times 10^6 \text{ g mol}^{-1}$, Sigma Aldrich) in a small amount ($< 20 \text{ mL}$) of Milli-Q water (Millipore) and stirred for 24 h; afterwards, the volume was adjusted to 20 mL. TBr-PHEA was used as photoinitiator, and a stock solution (25 mg mL^{-1}) was prepared in water. The DNA and TBr-PHEA concentrations of samples employed for microfabrication studies were 0.4 and 3.0 mg mL^{-1} , respectively.

TBr-PHEA was synthesized following our previously reported methodology,[12-13] starting from a chromophoric initiator, which structure and spectroscopy has been reported elsewhere [14]. Polymer chain length was evaluated by NMR and GPC, leading to a value $n=80$. Maximal absorption ($\lambda_{\text{abs}}=420 \text{ nm}$) and emission wavelengths ($\lambda_{\text{em}}=530 \text{ nm}$), molar extinction coefficient ($\epsilon \text{ ca } 40000 \text{ L}\cdot\text{mol}^{-1}\cdot\text{cm}^{-1}$), and luminescence quantum yield ($\phi=0.02$) were measured with a Jasco 670 UV-Visible spectrophotometer and a Horiba-Jobin Yvon Fluorolog-3® spectrofluorimeter equipped with a red sensitive Hamatsu R-928 detector, respectively. Singlet oxygen generation efficiency ($f=0.68$) was evaluated from a diluted solution of TBr-PHEA in chloroform, using the same methodology as reported in details before [15]. An aqueous stock solution of TBr-PHEA in water (25 mg mL^{-1} , $\text{ca } 1 \text{ mmol}$) was prepared with a freshly synthesized batch of TBr-PHEA and immediately after that stored in the fridge at $4 \text{ }^\circ\text{C}$.

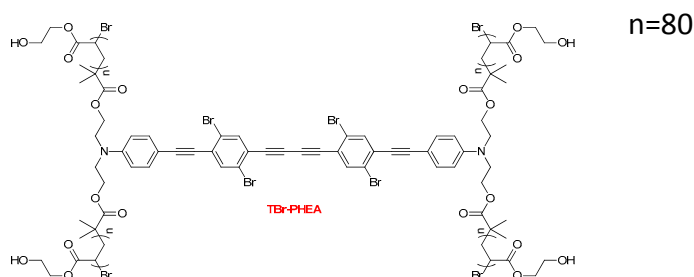


Figure 1: TBr-PHEA singlet-oxygen generator for two-photon induced cross-linking of DNA at 532 nm.

- Photosensitive BSA solutions:

Albumin from bovine serum (BSA Fraction V, pH = 6.9, 98%; UniRegion Bio-Tech, US) and photoinitiator riboflavin (RB; Merck Millipore, German) from *Eremothecium ashbyii* were obtained from Sigma-Aldrich® and used without any previous purification. 400 mg mL^{-1} of BSA was mixed with 1 mL of RB $1 \times 10^{-3} \text{ mol L}^{-1}$ solution in Milli-Q water (Millipore, USA) and at $4 \text{ }^\circ\text{C}$. Next, 0.5 mL of triethanolamine 0.1 mol L^{-1} (TEA; $\text{N}(\text{CH}_2\text{CH}_2\text{OH})_3$; Merck Millipore, German or from J. T. Baker®) was employed as a co-initiator. The solutions were stored at 0 to $4 \text{ }^\circ\text{C}$.

Solution of gelatine was prepared by mixing 120 mg of gelatin with 1 mL of eosin Y $10 \text{ mmol L}^{-1} \text{ C}_{20}\text{H}_6\text{Br}_4\text{Na}_2\text{O}_5$, C.I. 45380 (Merck KGaA, German) at $\geq 70 \text{ }^\circ\text{C}$ and then 0.5 mL of TEA was added.

2.2 Photochemistry characterizations

- ATR-FTIR spectroscopy

Fourier transform infrared (FTIR) spectra were recorded with a Perkin-Elmer Frontier FTIR spectrometer using a universal attenuated total reflectance (ATR) sampling accessory. Four scans were accumulated for a sample in $4000 - 600 \text{ cm}^{-1}$ spectral range with a resolution of 4 cm^{-1} . Background spectrum was collected before a measurement. A small drop ($10 \text{ } \mu\text{L}$) of the samples was placed on the ATR accessory and dried for 60 min at room temperature, resulting in DNA-Tr-PHEA layer with thickness less than 0.5 mm . A blue LED (455 nm , 300 mW cm^{-2} , THORLAB) was used as excitation source. The samples were irradiated for 30 min.

- Fluorescence spectroscopy

Fluorescence measurements were obtained with a Hitachi F-4500 spectrofluorimeter, using front-face fluorescence with slit widths of 5 nm for excitation and emission. The samples were excited at 320 nm and the spectra were registered from 330 to 600 nm. Solutions (180 μ L) with and without TEA were placed between two quartz discs support in a Teflon® cell and irradiated with above mentioned blue LED for 30 min. The spectrum of non-irradiated sample was subtracted from irradiated one.

2.3 Two-photon 3D microfabrication set-up and method

The experimental set-up is based on a commercial two-photon 3D microfabrication machine (Teem Photonics Inc.) using a Q-switched Nd:YAG microchip laser generating sub-nanosecond green pulses at 12 kHz repetition rates (Figure 2). The laser beam is focused on the sample with a microscope objective (x100, NA=1.3). During the fabrication, the sample is translated through the laser focus by a 3-axis piezoelectric stage. The fabrication contours are calculated by a dedicated software, which also controls the fabrication parameters, i.e., laser power, exposure time, and 3D positioning.



Figure 2: Two-photon 3D microfabrication machine.

The photosensitive DNA material was obtained by evaporation of water from a DNA/TrBr-PHEA drop on a microscope glass slide (25 \times 25 mm). It had a final diameter around 5 mm and a thickness of less than 50 μ m. The microfabrication was performed in the edge of the drop. The average laser power was in the milliwatt range, the irradiation exposure time was 10 ms, and the voxel distance was 0.12 micron.

2.4 DLP stereolithography 3D printing set-up and method

3D printing tests of BSA and gelatine were done with a modified commercial DLP stereolithography printer (Titan 1 from Kudo 3D) based on a ViewSonic DLP® projector PJD7820HD (3,000 ANSI lumens). The initial image size was reduced to 2 \times 3.5 cm² by using an additional lens. A thermalized water tank was added to control the sample container temperature that was of 70 to 80 °C range for gelatin. A glass microscope slide was glued on a build platform to make easier the binding of protein-based objects. A cellulose acetate foil was used as an anti-binding layer at the bottom of the sample container.

The optimization of photo-cross linking was obtained by the 2D irradiation of a “star” test image into a circular pool (1cm diameter, 1 mm high) of sample solution (~0.5 mL) at room temperature. The 3D structure of gelatine with the DLP printer was obtained in a sample volume of 10 mL. After irradiation, BSA was developed with water at room temperature and gelatine with water at 75 °C.

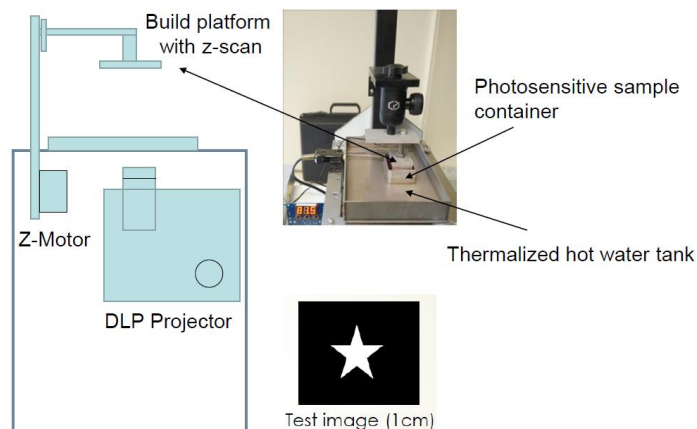


Figure 3: Modified commercial DLP stereolithography printer used to test the fabrication of protein-based 3D objects.

3. RESULTS AND DISCUSSIONS

3.1 Spectroscopy of photo-induced crosslinking

3.1.1 ATR-FTIR spectroscopy of DNA crosslinking

The FTIR spectra of DNA in presence of photoinitiator, before and after 30 min of irradiation, are shown in Figure 4. DNA spectra show peaks at 1695, 1646, 1607, and 1484 cm^{-1} that can be attributed to guanine, thymine, adenine, and cytosine nucleobases, respectively. It is possible to observe that with increasing irradiation times the bands at 1695 and 1646 cm^{-1} decrease, suggesting a photo-induced interstrand crosslinking of DNA. [16] DNA crosslinking is believed to occur by singlet oxygen ($^1\text{O}_2$) mechanism. After excitation of the photoinitiator to the triplet excited state, a transfer of energy to the ground state of triplet molecular oxygen can occur, generating the $^1\text{O}_2$. Then, this singlet oxygen can react with the thymine and guanine groups present in DNA to form the interstrand DNA crosslinking.

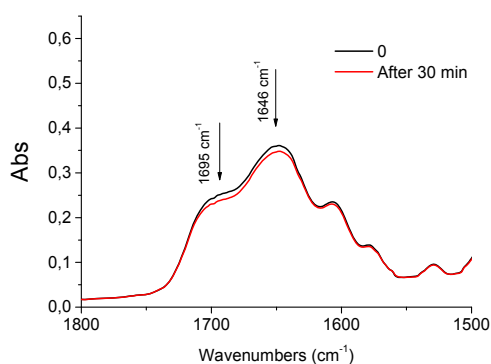


Figure 4: FTIR spectra of DNA solution 0.4 mg mL^{-1} in the presence of photoinitiator before and after 30 min of irradiation by a blue LED (455 nm, 300 mW cm^{-2}).

3.1.2 Fluorescence spectroscopy of BSA crosslinking

Figure 5 shows differential emission spectra of BSA 400 mg mL^{-1} and RB $2 \times 10^{-3} \text{ mol L}^{-1}$ solutions as function of the irradiation time. RB emission band is centered at 530 nm and decreases as function of the irradiation time due to the photobleaching process. Simultaneously, a new band centered at 450 nm grows during the irradiation process. It can be attributed to the tyrosine dimer (dityrosine) formation during the inter-protein cross-linking. [17] Similarly to the DNA

crosslinking mechanism, RB can generate singlet oxygen that can react through hydrogen removal (type I) from oxidizable amino acid residue (tyrosine) of the protein, making a covalent bond. [18] On the other hand, TEA acts as a co-initiator and electron donor to RB (type II) to facilitate a photo-crosslink process. [19]

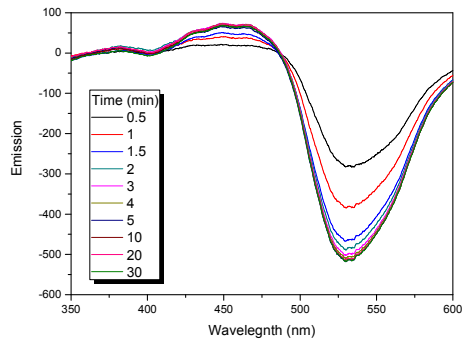


Figure 5: Corrected fluorescence spectra ($\lambda_{exc} = 320 \text{ nm}$) of an aqueous BSA solution (400 mg mL^{-1}) and RB ($2 \times 10^{-3} \text{ mol L}^{-1}$) irradiated by a blue LED (455 nm , 300 mW cm^{-2}) for 0.5 to 30 min. The non-irradiated solution spectra were subtracted from irradiated ones.

3.2 Two-photon 3D microfabrication of DNA

Figure 6 shows examples of SEM micrographs of DNA microstructures obtained by scanning a laser beam. In Figure 6a, one can see ten parallel lines resulting of the two-photon induced DNA cross-linking. These lines were fabricated with regular, smooth, and reproducible characteristics. The fabrication of 3D micro-lens of DNA on the surface of microscope cover glass is show in Figure 6b, demonstrating the potential of DNA to be used in micro-optics applications. The micro-lens was fabricated by one shell slicing 3D method with $10 \mu\text{m} \times 2 \mu\text{m}$ size (Figure 6c).

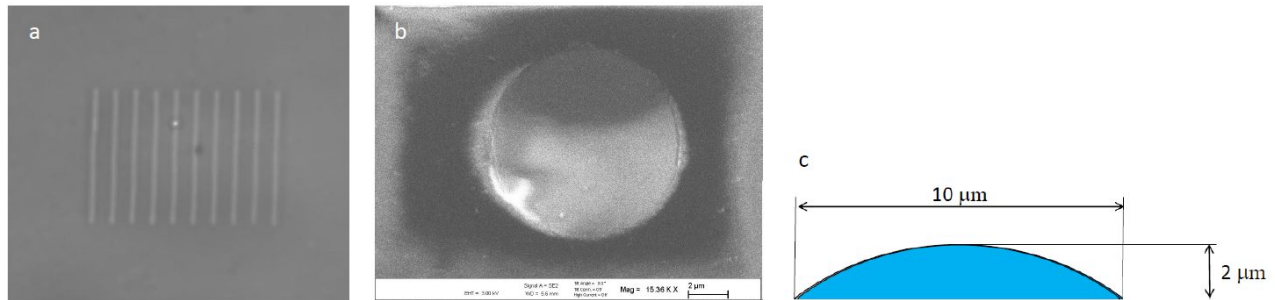


Figure 6: SEM micrograph of parallel lines (a), micro-lens from DNA crosslinking (b), and 3D micro-lens structure model (c).

3.3 DLP 3D printing of BSA and gelatine

Figure 7 shows photos of an optimization process by irradiation (10 mn) of a “star” test image. During irradiation, a strong fluorescence is emitted by photo-initiators (Fig. 7a), that after become photobleached, and a more transparent region appears (Fig. 7b). A development is done in hot or cold water for gelatine and BSA, respectively (Fig. 7c). As one can see in Fig. 7d, gelatine “star” is well formed with a homogeneous thickness of 1mm. However, the same test with BSA led only to a partial polymerization of the “star shape” with an inhomogeneous thickness, which is seen in Fig. 7e.

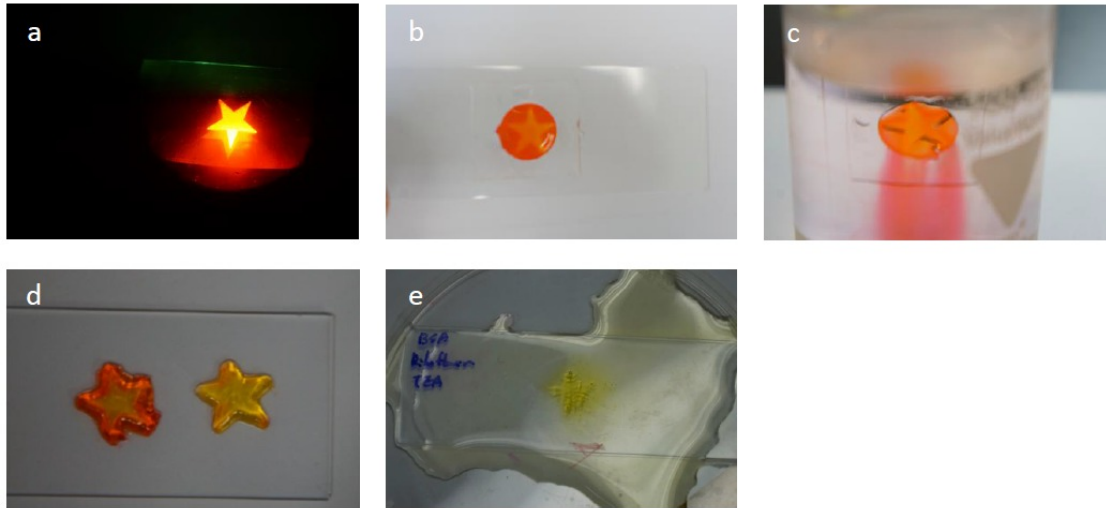


Figure 7: (a) photo-initiator fluorescence during irradiation (10 mn), (b) just after irradiation, (c) development in water, (d) typical results for gelatine with Eosin Y (left), and Robiflavin (right), (e) “best” result for BSA.

Preliminary tests of 3D printing of gelatine were performed by a projection of two layers of “square” images, as shown in Fig. 8. The distance between layers was 800 μm , and the exposure time 10 mn. After development, one can clearly distinguish the two layer morphology on a binding background that is automatically generated by the 3D printer.

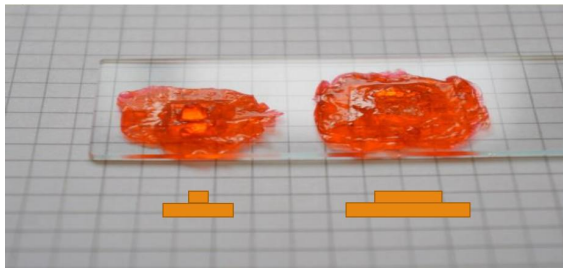


Figure 8: Preliminary tests of 3D printing two layers of “square” images with gelatine.

4. CONCLUSIONS

We have demonstrated an efficient interstrand crosslinking of DNA by means of a light excitation of a singlet oxygen generator. Using the two-photon induced crosslinking technique, we have obtained a 3D DNA microlens, which opens the way for using DNA material in micro-optics application.

We have also presented our preliminary results on using a commercial 3D printer based on a video projector to polymerize slicing layers of gelatine-objects. The 3D printing of natural organic materials by photochemistry methods is a new approach that should lead to higher resolution 3D structures than extruding process. This is a new step towards the development of 3D printing for biomedical applications, and more generally for green, 3D water-based processes.

5. ACKNOWLEDGEMENTS

In Brazil, the work was funded by a Special Visiting Researcher Fellowship under the Brazilian Scientific Mobility Program “Sciences without border” CNPQ grant 314496/2014-9. In Taiwan, it was supported by the Ministry of Science and Technology (MOST 103-2633-E-166 -001).

REFERENCES

1. J. D. Pitts, P. J. Campagnola, G. A. Epling, and S. L. Goodman, "Reaction efficiencies for sub-micron multi-photon freeform fabrications of proteins and polymers with applications in sustained release," *Macromolecules* **33**, 1514-1523 (2000).
2. Kaehr B, Allen R, Javier DJ, Currie J, Shear JB Guiding neuronal development with in situ microfabrication. *Proc Natl Acad Sci USA* 101:16104–16108 (2004).
3. Iosin M, Stephan O, Astilean S, Duperray A and Baldeck PL, "Microstructuring of protein matrices by laser induced photochemistry," *J. Optoelectron. Adv. Mater.* 9(3), 716-720 (2007).
4. Iosin M, Scheul T, Nizak C, Stephan O, Astilean S and Baldeck P, "Laser microstructuring of three dimensional enzyme reactors in microfluidic channels," *Microfluid. Nanofluid.* 10(3), 685-690 (2011).
5. Lin, C. L., Pan, M. J., Chen, H. W., Lin, C. K., Lin, C. F., & Baldeck, P. L.. Laser cross-linking protein captures for living cells on a biochip. In *SPIE BiOS* (pp. 93100D-93100D). (2011).
6. Baldeck, P. L., Scheul, T., Bouriau, M., Stephan, O., Malval, J. P., Lin, C. L., ... & Chung, T. T. (2011, September). Nonlinear photochemistry and 3D microfabrication with Q-switched Nd: YAG microchip lasers. In *SPIE Photonic Devices+ Applications* (pp. 811309-811309). (2011).
7. Baldeck, P. L., Prabhakaran, P., Liu, C. Y., Bouriau, M., Gredy, L., Stephan, O., ... & Lin, C. L. (2013, September). Recent advances in two-photon 3D laser lithography with self-Q-switched Nd: YAG microchip lasers. In *SPIE Organic Photonics+ Electronics* (pp. 88270E-88270E). (2013)
8. Lin, Chuen-Fu; Lin, Che-Kuan; Liu, Yi-Jui; Chiang, Chung-Han; Pan, Ming-Jeng; Baldeck, PL ; Lin, Chih-Lang Laser-induced cross-linking GFP-AcmA' bioprobe for screening Gram-positive bacteria on a biochip RSC ADVANCES 2014 ; 4 (108) 62882-62887
9. J. Grote, J. Hagen, J. Zetts, R. Nelson, D. Diggs, M. Stone, P. Yaney, E. Heckman, C. Zhang, W. Steier, A. Jen, L. Dalton, N. Ogata, M. Curley, S. Clarson, and F. Hopkins, "Investigation of Polymers and Marine-Derived DNA in Optoelectronics," *J. Phys. Chem. B*, 108, pp. 8584-8591, (2004).
10. Lewis E. Johnson, Luke N. Latimer, Stephanie J. Benight, Zachary H. Watanabe, Delwin L. Elder, Bruce H. Robinson, Carrie M. Bartsch, Emily M. Heckman, James Grote, "Novel cationic dye and crosslinkable surfactant for DNA biophotonics." *Proc. SPIE*, 8464, 84640D, 2012.
11. F. Ouchen, P. Yaney, A. Lesko, E. Heckman and J. Grote, "Effect of UV Crosslinking of DNA-CTMA Biopolymer on its Electrical and Optical Properties", *SPIE Proceedings*, 8817(10), (2013).
12. Monnereau, C., S. Marotte, P.-H. Lanoe, O. Maury, P. Baldeck, D. Kreher, A. Favier, M.-T. Charreyre, J. Marvel, Y. Leverrier, and C. Andraud (2012). "Water-soluble chromophores with star-shaped oligomeric arms: synthesis, spectroscopic studies and first results in bio-imaging and cell death induction." *New J. Chem.* 36(11): p. 2328-2333.
13. Massin, J., A. Charaf-Eddin, F. Appaix, Y. Bretonniere, D. Jacquemin, B. van der Sanden, C. Monnereau, and C. Andraud (2013). "A water soluble probe with near infrared two-photon absorption and polarity-induced fluorescence for cerebral vascular imaging." *Chem. Sci.* 4(7): p. 2833-2843.
14. Gallavardin, T., C. Armagnat, O. Maury, P.L. Baldeck, M. Lindgren, C. Monnereau, and C. Andraud (2012). "An improved singlet oxygen sensitizer with two-photon absorption and emission in the biological transparency window as a result of ground state symmetry-breaking." *Chem. Commun.* 48(11): p. 1689-1691.
15. Lanoe, P.-H., T. Gallavardin, A. Dupin, O. Maury, P.L. Baldeck, M. Lindgren, C. Monnereau, and C. Andraud (2012). "Influence of bromine substitution pattern on the singlet oxygen generation efficiency of two-photon absorbing chromophores." *Organic & Biomolecular Chemistry.* 10(31): p. 6275-6278.
16. Cadet, J. and J. R. Wagner (2013). "DNA Base Damage by Reactive Oxygen Species, Oxidizing Agents, and UV Radiation." *Cold Spring Harbor Perspectives in Biology* 5(2).
17. Kampf, C. J., F. B. Liu, K. Reinmuth-Selzle, T. Berkemeier, H. Meusel, M. Shiraiwa and U. Poschl (2015). "Protein Cross-Linking and Oligomerization through Dityrosine Formation upon Exposure to Ozone." *Environmental Science & Technology* 49(18): 10859-10866.
18. Thomas, A. H., B. N. Zurbano, C. Lorente, J. Santos, E. A. Roman and M. L. Dantola (2014). "Chemical changes in bovine serum albumin photoinduced by pterin." *Journal of Photochemistry and Photobiology B-Biology* 141: 262-268.
19. Kim, S. H. and C. C. Chu (2009). "Visible light induced dextran-methacrylate hydrogel formation using (-)-riboflavin vitamin B2 as a photoinitiator and L-arginine as a co-initiator." *Fibers and Polymers* 10(1): 14-20.